Innovative Control Effectors for Maneuvering of Air Vehicles

AUTHOR Georgi Hristov
FACULTY ADVISOR Professor David Williams

Abstract

Flow control is a rapidly developing key technological area which is subject to extensive research as it offers the potential to enhance aircraft aerodynamic performance, control, and maneuverability. The current paper details the methods and the results of a research which envisions assisting the newly formed NATO Task Group STO-AVT-239, with assessing the ability of modern active flow control actuators to improve the performance of Unmanned Combat Air Vehicles (UCAV). The project was supported by the ACE Undergraduate Research Topics Program at IIT and investigated the feasibility of the Coanda effect in achieving Circulation Control (CC) in order to produce rolling motion in cruise.

Understanding of the performance of the SACCON airframe design and the complex vortex dominated flow field around was achieved through research papers and previous work of NATO Task Groups. It was discovered that a mid-span vortex influences and disturbs the flow above the control surfaces diminishing their effectiveness. A simple freeware computer code was used to predict the behavior of the airframe and the results were compared to experiment. The predictive abilities of the code were assessed to be good given the limitations of the software. Along with the airframe, CC was researched in order to predict its maneuver control capabilities. The experimental data and the computational predictions were then used in combination with a semi-empirical aileron control model to predict the aileron effectiveness and compare it to the CC results. In order to be able to apply for research funding from appropriate institutions, a windtunnel experiment was designed and planned to be conducted to validate the developed model.

Introduction

Flow control implements the ability of small-scale devices to produce large-scale changes in aerodynamic flows. Research activities in the area include the fluid mechanics analysis of synthetic jet actuators, pneumatic blowing, active dimples, plasma actuators, circulation control, etc. and their application to existing and novel vehicle configurations aiming to reduce skin friction and pressure drag, delay boundary layer separation, and enhance lift.

In this report we focus on Circulation Control and its application to the investigated airframe. Circulation Control technologies have been around since the early 1930s and have been successfully demonstrated to produce lift threefold over airfoils with flaps. Extensive research has been done in the area with main focus on increasing the lifting force at times when large lifting forces at slow speeds are required, such as take-off and landing [Ref. 1]. In recent years, circulation control has been used as a maneuver performance enhancement method aiming to replace conventional control surfaces because of disadvantages such as high mechanical complexity due to the necessity to withstand heavy mechanical loads and hinge moments, reduced volume available for fuel storage, increased structural weight, and increased radar signature. A work by Manchester University led to the FLAVIIR Demon UAV project in collaboration with Cranfield University and BAE Systems [Ref. 1]. This was the first UAV to employ circulation control techniques and to successfully achieve control in cruise. This project proved that the circulation control can replace conventional control surfaces and motivated further research in the field.

The current research project intended to assist a newly formed NATO Task Group STO-AVT-239, with assessing the ability of modern active flow control actuators to improve the performance of Unmanned Combat Air Vehicles (UCAV). The project intended to acquire, analyze, and process data relevant to the control and maneuverability of UCAV aircraft for the duration of the ACE Undergraduate Research Topics Program as part of the “Security” topic of the IIT Engineering Themes.

The airframe under investigation was a generic UCAV called SACCON (Fig. 1) which is an acronym for Stability And Control Configuration.

It was designed by NATO STO-AVT-161 and NATO STO-AVT-201 task groups to explore the stability and control characteristics of medium sweep delta wing UAVs. Extensive experimental data was obtained in wind tunnels in Germany, France, and the U.S. At the same time state-of-the-art computer simulations were done at the U.S. Air Force Academy and several other locations in England, France, and Germany.

The objectives of the current research were to:

1) Obtain an understanding of the performance and control issues of the SACCON design. In particular, at high angles of attack, there is strange lift and moment coefficient behavior that is associated with a mid-span longitudinal vortex.

2) Investigate the extent that the simple freeware code XFLR5 can predict SACCON performance.

3) Predict if conventional ailerons can be replaced by circulation control (Coanda effect) actuators. Conventional aileron control surfaces lose effectiveness in some angle of attack range, because of cross flow effects from the mid-span vortex. A solution to the problem would also require knowledge on how much power (or flow) from the aircraft engine would be needed to produce a roll moment that is equivalent to the conventional ailerons.

4) Design an experiment that will test the validity of the predicted performance of circulation control actuators.

The approaches taken to find solutions to these objectives are described in the following section.

Methods

A. Review of Research Papers and Journals

The research was founded on previous investigations, and created a model for predicting the parameters necessary for SACCON to achieve roll motion equivalent to ailerons with circulation control wing.

SACCON – the airframe used in the project (Fig. 2) – is a delta wing planform with medium sweep leading edges – 53˚. SACCON has been investigated by several successive NATO Task Groups, and thus there is extensive informa-

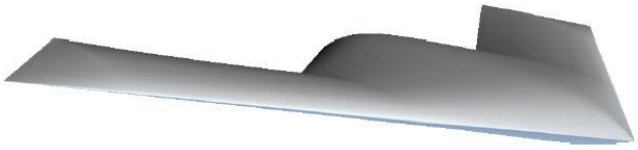

Figure 1. *SACCON airframe rendering [Ref. 2].*

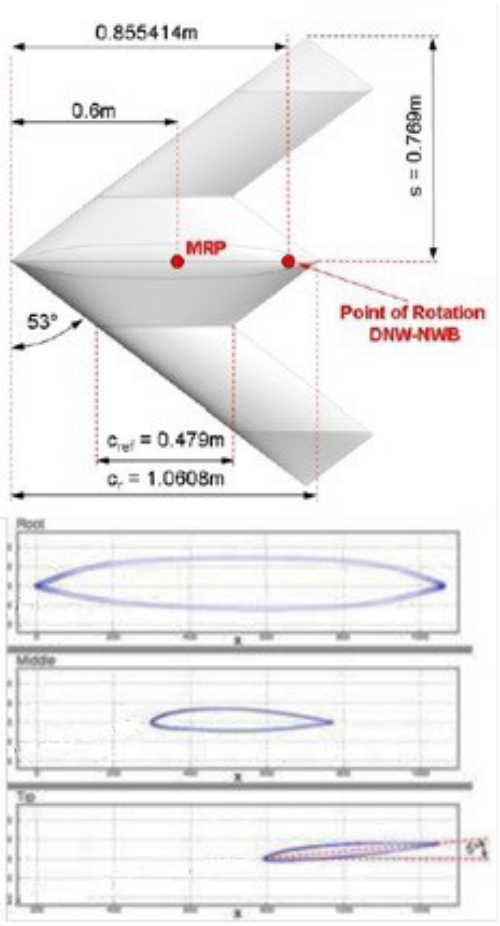

Figure 2. *SACCON geometry [Ref. 3].*

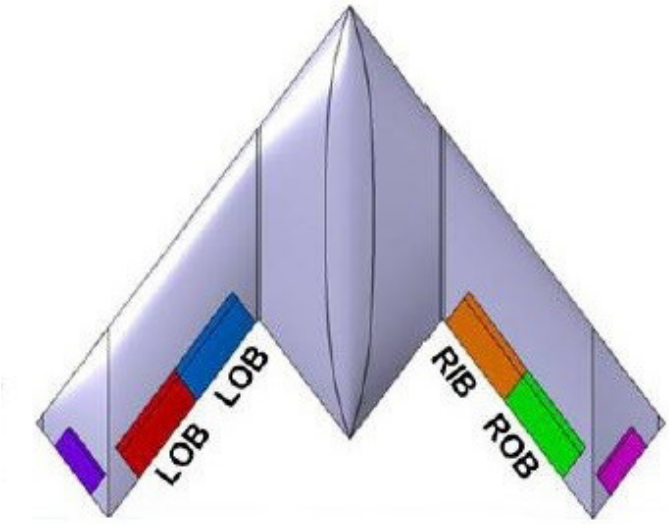

Figure 3. *Control surfaces on SACCON [Ref. 4].*

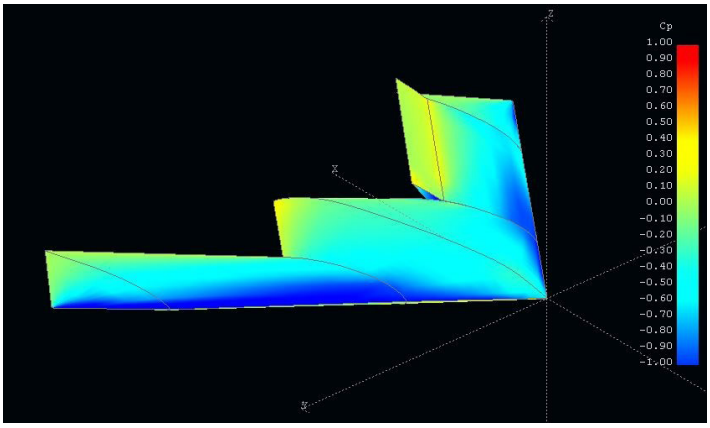

Figure 4. *SACCON XFLR5 image.*

tion on its performance from windtunnel tests. The findings from the NATO STO-AVT-161 and NATO STO-AVT-201 were used to model the airframe and collect the necessary information for its roll behavior due to ailerons. Information from static windtunnel tests was collected for SACCON with and without ailerons. Several configurations with ailerons were designed. The ailerons spanned most of the main wing (as seen in Fig. 3), and was split in half to inboard and outboard aileron. For convenience purposes the left and right inboard control surfaces were called LIB and RIB ailerons respectively; the left and right outboard control surfaces were called LOB and ROB ailerons respectively and the full left and full right control surfaces were called LIBLOB and RIBROB ailerons. This notation was used throughout the paper to indicate the control surface in question.

B. Computational Model

Aerodynamic data for roll performance was needed for the investigation. Simple and fast aerodynamic computational software called XFLR5 was used to numerically simulate the airframe and obtain performance data of the SACCON airframe. XFLR5 is a free analysis tool for airfoils, wings and planes operating at low Reynolds numbers, which was chosen for the initial airframe analysis due to its simplicity and ability to produce good results. The software is based on the inviscid and incompressible potential flow theory, so it cannot predict the mid-span vortex which is characteristic of the flow around SACCON at high angles of attack. However, this was not considered critical for the goals of the project. For investigating compressible flows, a compressibility correction is included; viscous drag can optionally be considered. XFLR5 included wing design capabilities based on the Lifting Line Theory, on the Vortex Lattice Method (VLM), and on 3D Panel Method.

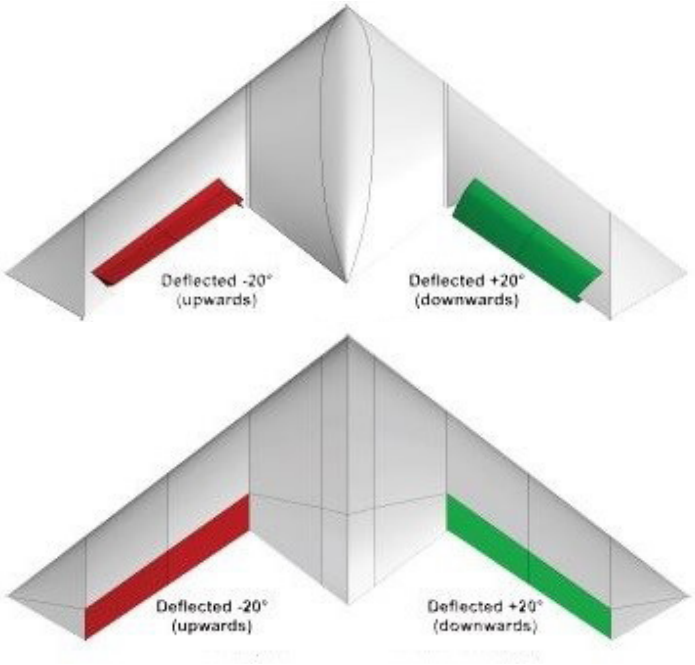

Figure 5. *Wind tunnel model geometry (Top) vs. XFLR5 geometry (Bottom) . Images: [Ref. 2].*

3D Panel Method and VLM were used to numerically simulate the airframe. The 3D Panel Method models the wing as a thick surface, whereas VLM is based on a simplified skeleton theory (also called camberline theory). In this method, the 3D surface is reduced to a set of infinitely thin sheet of vortices on the mean camber line, hence neglecting all effects coming from thickness, to compute lift and induced drag. Further simplifications of the methods include limitation to low Reynolds numbers and inability to predict stall.

Due to the guidelines of the XFLR5 software and the specific limitations (described in the Results section) related to each method, a 3D Panel Method was used for Cp predictions and VLM was preferred for moment calculations.

The accuracy of the results was a consideration while modeling SACCON's medium sweep configuration. It is obvious that the simple theory behind these methods is not able to model the complex vortex systems occurring for such aircraft, especially at higher angles of attack. However, the use of XFLR5 is justified because the prime interest of the research is in control during cruise conditions at low angles of attack where there is no separation, and little vortex effects. On the other hand, the simple potential flow theory is known to behave conservatively in most cases,

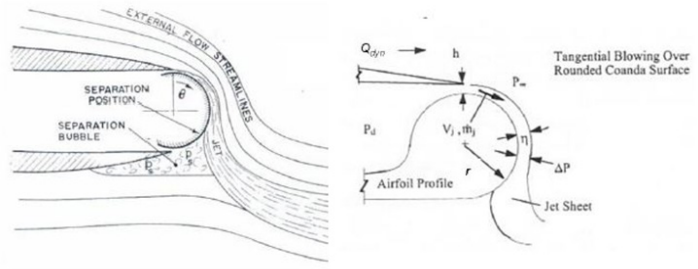

Figure 6. *Coanda effect image [Ref. 5 and 6].*

meaning that the calculated loads are expected to be typically larger than what really will appear at the aircraft, and the actual control surface efficiencies are expected to be much lower than predicted. Thus, the range of flight parameters for which XFLR5 is useful was determined.

The control surface definition used for XFLR5 is not able to model the geometry from the windtunnel exactly. The simplification which was used even led to slightly bigger control surfaces and was expected to produce a small over-prediction of control surface effects (Fig. 5).

C. Circulation Control

Circulation control is one of the most promising flow control techniques to provide direct control of lift. It employs the Coanda effect and involves virtual aerodynamic shape change as opposed to a real mechanical shape change. The Coanda effect is the tendency of a moving fluid to attach itself to a surface (called Coanda surface) and flow along with it (Fig 6). The phenomenon is explained as the result of entrainment of stationary ambient fluid around the moving fluid jet. In one application, the Coanda effect is used for circulation control in order to influence lift especially at high angles of attack when the flow would otherwise separate (stall). When the jet sheet of air with a higher velocity than the free stream is blown over the upper surface of an airfoil, the jet remains attached to the Coanda surface, because of the balance between the sub-ambient pressure within the jet flow and the centrifugal force felt on the curved surface . As an effect of the increasing jet velocity, the rear stagnation point moves forward on the lower trialing edge inducing an effective camber, thereby increasing circulation around the wing and lift.

The first phase of the design process of a circulation control wing requires sizing of the span, slot area and jet momentum blowing coefficient. The aerodynamic performance of a circulation control device is closely related to the momentum blowing coefficient (Equation 1) which characterizes the energy introduced to the flow by the Coanda jet.

$$C_\mu = \frac{\dot{m}_j V_j}{q S_w} \qquad \text{Eq. 1}$$

where m_j is the jet mass flow rate, V_j is the jet exit velocity, S_w is the wing area, and $q=0.5\rho_\infty V_\infty^2$ is the dynamic pressure. The dynamic pressure is a function of the free stream air density ρ_∞, and the free stream velocity V_∞.

Circulation Control (CC) effectors' scaling was based on an empirical control response model described in reference [7]. Equation 2 is a curve fit to experimental data from Englar [Ref. 5]. This relationship presents the change of lift due to blowing as a function of the velocity ratio V_j/V_∞. At a constant slot height to chord ratio h/c, the lift augmentation increases linearly with V_j/V_∞..

$$\Delta C_L = 40\left(\frac{h}{c}\right)^{0.64}\left(\frac{V_j}{V_\infty} - 1\right) \qquad \text{Eq. 2}$$

The CC effector's efficiency is characterized by the incremental lift coefficient increase with increment in blowing coefficient. This value is known as lift augmentation and its magnitude is typically in the region of 15 to 60 [Ref. 8].

$$Lift\ augmentation = \frac{\partial C_L}{\partial C_\mu} \qquad \text{Eq. 3}$$

Besides the sizing of the slot, the slot geometry at the trailing edge in terms of slot height and trailing edge radius also has a significant impact on achieved performance. The proposed range of geometric parameters where CC is most effective is shown in Figure 7.

D. CC Actuator and Aileron Modelling

The deflection of the conventional control surfaces on aircraft, such as ailerons, generates change in lift on the wing and in turn produces a rolling moment. Thus a method for determining the rolling moment induced by an aileron is to model roll response as a function of change of lift on the wing. Similarly, the rolling moment induced by a circulation control system can be determined using the increment in lift over the wing as a function of the blowing coefficient [Ref. 8].

The non-dimensional control derivative

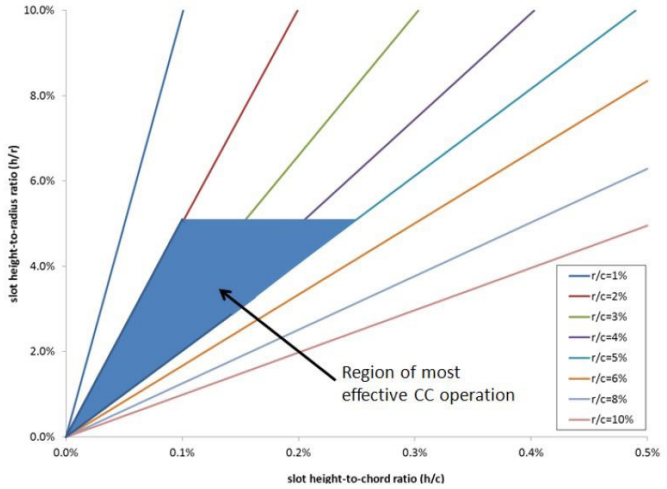

Figure 7. *Region of most effective CC operation [Ref. 9 and 10].*

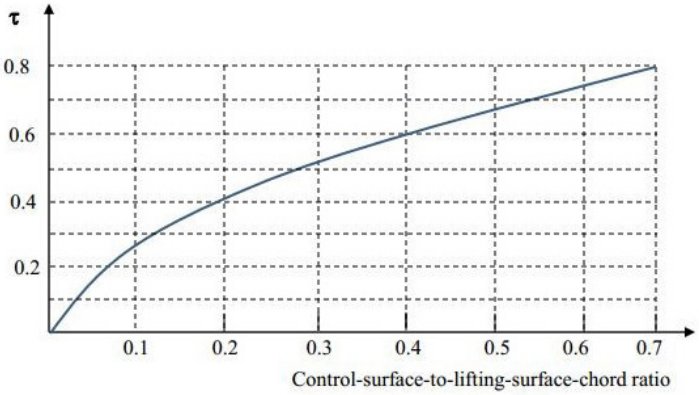

Figure 8. *Aileron effectiveness parameter τ [Ref. 11].*

$C_{l\delta} = dC_l/d\delta$, where δ is aileron deflection angle, is a measure of the roll control authority of the aileron. It represents the change in rolling moment per unit change of aileron deflection. The larger the $C_{l\delta}$, the more effective the aileron is at creating a rolling moment. An estimate of the roll control power can be obtained by applying a simple 'strip integration method' [Ref. 11]:

$$C_l = C_L \frac{1}{Sb} \int_{y1}^{y0} c(y) y dy \qquad \text{Eq. 4}$$

where the parameters y0 and y1 represent the inboard and the outboard positions of the aileron with respect to the fuselage centerline. The parameter c(y) is the chord length as a function of the y-coordinate which goes along the span of the wing. In the case of SACCON, c(y) is a constant as the chord of the wing is constant in the region where the control surfaces are positioned. CL is the section lift coefficient, which is assumed to be constant over the wing span, on the section containing the aileron. It is defined as:

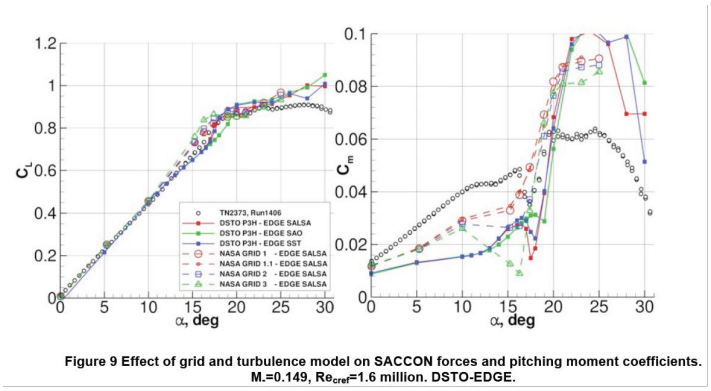

Figure 9 Effect of grid and turbulence model on SACCON forces and pitching moment coefficients. M.=0.149, Re_{cref}=1.6 million. DSTO-EDGE.

Figure 9. *SACCON lift, pitching moment, and rolling moment experimental results (no ailerons) [Ref. 12].*

$$C_L = C_{L\alpha}\alpha = C_{L\alpha}\frac{d\alpha}{d\delta}\delta = C_{L\alpha}\tau\delta = \frac{\partial C_L}{\partial \alpha}\tau\delta \qquad \text{Eq. 5}$$

where τ is the aileron effectiveness parameter and is obtained from Figure 8, given the ratio between aileron-chord and wing-chord.

The CC actuator modelling closely followed the method used in the Demon UAV [Ref. 1]. The Demon model used an analogous strip integration method:

$$C_{l_\delta} = \frac{\partial C_{LF}}{\partial \delta}\frac{1}{Sb}\int_{y1}^{y0} c(y) y dy \qquad \text{Eq. 6}$$

where the derivative is the rate of change of lift coefficient due to actuator deflection for full span trailing edge actuator. A part-span correction was applied to account for the actuator's limited extent along the wing:

$$\frac{\partial C_{LF}}{\partial \delta} = \frac{\partial C_L}{\partial \delta}\frac{S}{S_{eff}} \qquad \text{Eq. 7}$$

where Seff is the fraction of wing area ahead of the part span trailing edge slot.

For symmetric aircraft with no sideslip and no rudder deflection, the roll moment coefficient is linearly modelled as:

$$C_l = C_{l_\delta}\delta \qquad \text{Eq. 8}$$

This allows Equation 6 to be rewritten as:

$$C_l = C_{LF}\frac{1}{Sb}\int_{y1}^{y0} c(y) y dy \qquad \text{Eq. 9}$$

Since the current project employed a different type of actuator than the one used in Demon UAV, equation 6 had to be modified to match the main goal of the project – to determine the relationship between roll moment coefficient and the

corresponding momentum blowing coefficient . Thus the derivative , which is the rate of change of lift coefficient due to momentum blowing coefficient, was used to determine the roll moment as a function of the momentum blowing coefficient.

$$C_{l_{C_\mu}} = \frac{\partial C_{LF}}{\partial C_\mu} \frac{1}{Sb} \int_{y1}^{y0} c(y) y dy \qquad \text{Eq. 10}$$

Results

A. NATO AVT-161 and NATO AVT-201 Experimental Data

The experimental data from the SACCON aileron roll control tests will be presented in this section for a series of control surface deflections. The data was comprised of different tests of different models in different windtunnels for the goals of the NATO AVT-161 and AVT-201 task groups.

SACCON was originally designed without control surfaces. However, removable control surfaces were later designed for further investigation. The various control surfaces can be seen in Figure 3. The aileron deflection angle was decided to be δ=20˚ because significant changes in roll moment needed to be observed. Furthermore, 20˚ is probably the largest useful deflection angle beyond which the aileron loses effectiveness. The hinge line of the ailerons was placed at 75% of the reference chord length cref.

The static aerodynamic results for lift, pitching moment, and rolling moment were presented in Figure 9.

The static aerodynamic data exhibits non-linearity in the moment graph because of the vortex

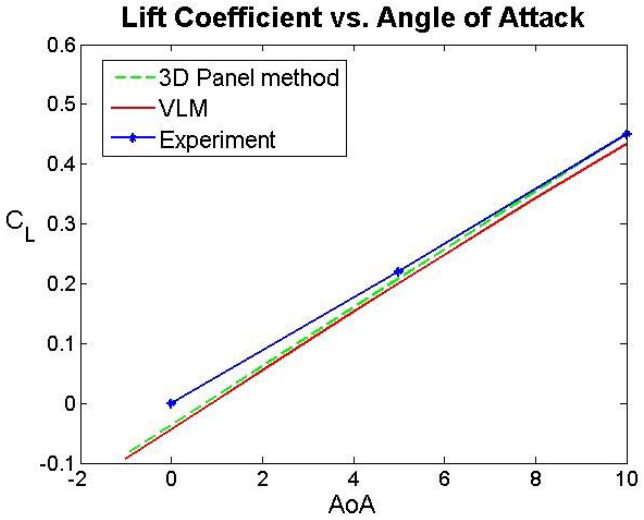

Figure 10. *XFLR5 computational results for lift coefficient versus angle of attack for SACCON.*

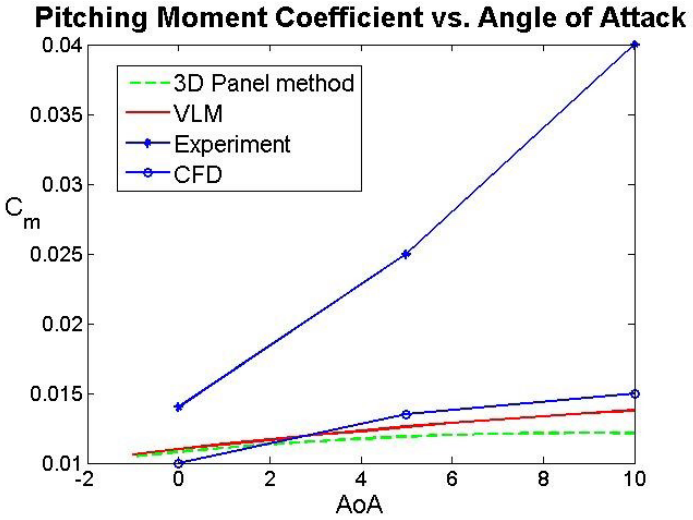

Figure 11. *XFLR5 computational results for pitching moment coefficient versus angle of attack for SACCON.*

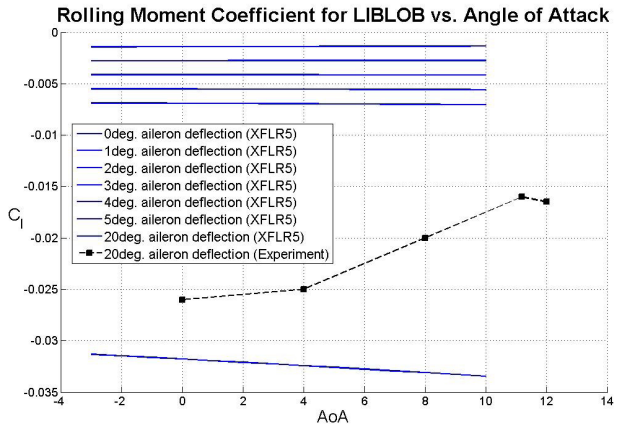

Figure 12. *XFLR5 computational results for the roll control authority of SACCON's full right aileron. Red lines are the XFLR5 predictions; Black dashed line is the experimental data.*

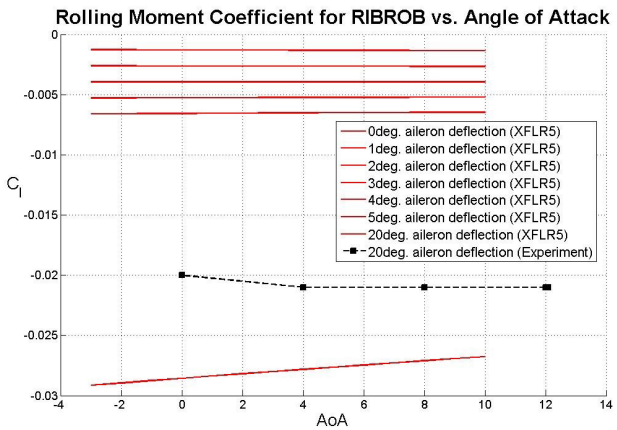

Figure 13. *XFLR5 computational results for the roll control authority of SACCON's full right aileron. Blue lines are the XFLR5 predictions; Black dashed line is the experimental data.*

structure that exists around SACCON. Attached flow exists along most of the span at low angles of attack. Small vortex separations form near the wing-tip and the nose of the vehicle along the sides of the body. As the angle of attack increases, the wing-tip vortex strengthens and moves further up the span of the wing. The flow from the nose, and around the body, also separates and rolls up into a secondary vortex. [Ref. 4]

The roll control authority of the ailerons was considered afterwards. Rolling moment data for aileron deflections was obtained from the NATO STO-AVT-201 Task Group. The experimental data for 20˚ LIBLOB and RIBROB aileron deflections was presented along with the computational results in Figures 12 and 13.

B. XFLR5 Computational Results

XFLR5 software was used to computationally estimate the performance of the SACCON airframe. The lift and pitching moment curves were used to compare the accuracy of the software against the experimental results. The Reynolds number (Re) and Mach number for the experimental data were 1.6 million and 0.149 respectively; the same numbers used in the XFLR5 simulation. Considering that 1.6 million is a relatively low Re, XFLR5 did not encounter any problems with the calculations. Both VLM and 3D Panel Method were used to model the flow field in the -1˚ to 10˚ angle of attack, and the results were presented in Figure 10 and Figure 11.

Both methods, when compared to each other, yielded similar to identical lift predictions, however, significant differences were observed in the pitching moment prediction. The XFLR5 results were then compared to the experimental data and CFD results from NATO STO-AVT-161. Discrete data points were taken from available experimental curves and plotted along with the computational results. The predicted lift curves from both methods were able to closely track the actual lift curve (Fig. 10). However, the pitching moment results were not satisfactory as they significantly differed from the windtunnel data (Fig. 11). Although noticeably different, VLM's predictions matched the experimental data better than the 3D Panel Method, and closely tracked some of the CFD results of the NATO task group. Therefore this method was chosen to be used in further moment calculations.

Rolling moment predictions at different aileron deflection angles were made using the VLM. The aileron deflections were chosen so that a negative rolling moment is produced; left aileron was deflected upwards and right aileron downwards. The computational predictions were made for full ailerons deflected at angles of 0˚ to 5˚, and 20˚ (top to bottom). Data points for 20˚ aileron angle of deflection were extracted from experimental data [Ref. 13] and then plotted along with the XFLR5 predictions (Fig. 12 and Fig. 13).

Aileron	Roll Moment			
	Experimental	Computational (XFLR5)	Semi-empirical	
			Using data from experiment	Using data from XFLR5
LIBLOB	-2.070E-02	-3.261E-02	-2.533E-02	-2.711E-02
RIBROB	-2.080E-02	-2.880E-02	-2.494E-02	-2.602E-02
LIB	-1.112E-02	-1.516E-02	-9.923E-03	-1.054E-02
RIB	-1.390E-02	-1.355E-02	-9.468E-03	-1.020E-02

Table 1. *Roll Moments Comparison from Experimental Data, Computational Data, and Semi-Empirical Model*

C. Roll equation validation

The experimental results and the XFLR5 predictions were used in Equation 4 to analytically predict the roll moment due to ailerons. The analytical predictions were then compared to the experimental data and the XFLR5 results for roll moment coefficient (Table I).

The error in the computational and the analytical predictions was calculated with respect to the experimental data results (Table II).

Figure 14 shows a graph that compares experimental data for simultaneous deflection of LIBLOB and RIBROB ailerons to advanced CFD software roll moment predictions. Both ailerons were deflected by 20˚ such that a negative rolling moment is produced.

The comparison between the experiment and the CFD code shows that in the region 0˚-10˚ angle of attack, the error in the CFD prediction varies

Aileron	Error in Roll Moment Prediction		
	Computational (XFLR5)	Semi-empirical	
		Using data from experiment	Using data from XFLR5
LIBLOB	57.5%	22.4%	31.0%
RIBROB	38.5%	19.9%	25.1%
LIB	36.3%	10.8%	5.2%
RIB	2.5%	31.9%	26.6%

Table 2. *Error in Roll Moments Calculations with Respect to Experimental Data*

between 60% and 40%.

D. Circulation Control Roll Control Authority

The main considerations in the design of the Circulation Control slot were to minimize the pressure drag and maximize the momentum blowing coefficient. To achieve maximum momentum blowing coefficient, the jet mass flow rate has to be maximized; thus maximizing the jet exit velocity and the blowing slot size. However, a higher slot size would result in a thicker trailing edge which in turn would result in a higher pressure drag penalty. Decreasing, the slot size would require increasing the jet exit velocity in order to maintain a constant momentum blowing coefficient. However, a velocity limit of Mach 1 exists, since subsonic flow is desired in order to avoid shocks. Also, although a supersonic wall jet can achieve circulation control, a significant portion of its momentum would be lost to wall shear [Ref. 7]. These conditions impose some restrictions in the design in terms of manufacturability of the slot, and limitations in the jet exit velocity.

Calculations of the momentum blowing coefficient necessary to achieve given rolling moment for various slot sizes were made (Fig. 15). It was established that the smaller the slots achieve higher roll moments compared to the bigger slots for a fixed momentum blowing coefficient. Based on this, the slot size was decided to be 0.003m. This slot size gives flow at Mach 0.95. The Coanda surface radius was chosen to be 0.06m so that the slot size is 5% of the radius. This was based

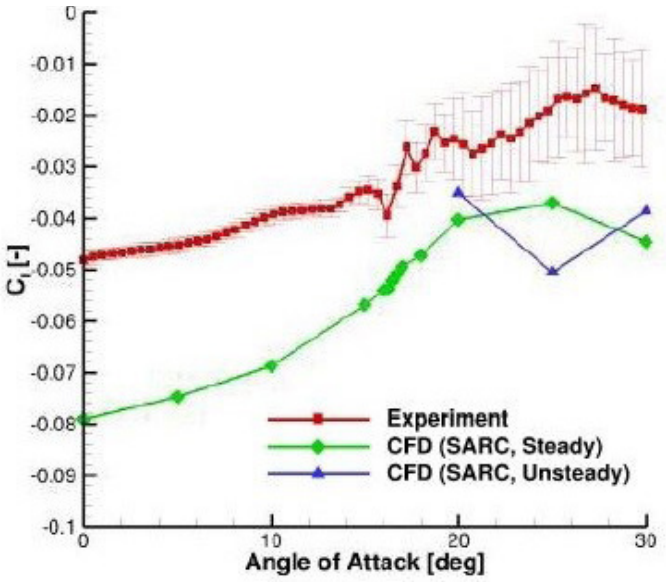

Figure 14. *Roll moment coefficient comparison between experimental data and advanced CFD code for LIBLOB and RIBROB ailerons simultaneously deflected by 20° [Ref. 4].*

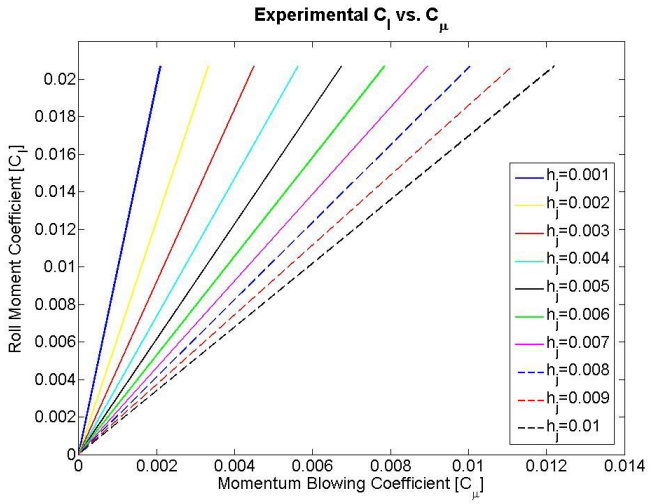

Figure 15. *Cl vs. Cμ for various slot heights (hj) based on experimental results.*

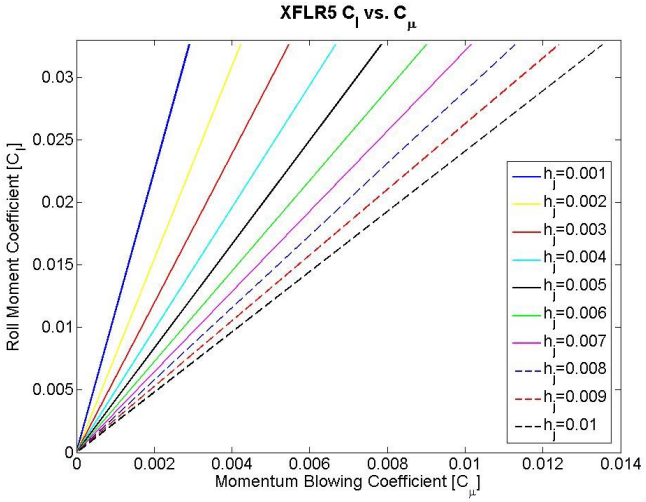

Figure 16. *Cl vs. Cμ for various slot heights (hj) based on XFLR5 results.*

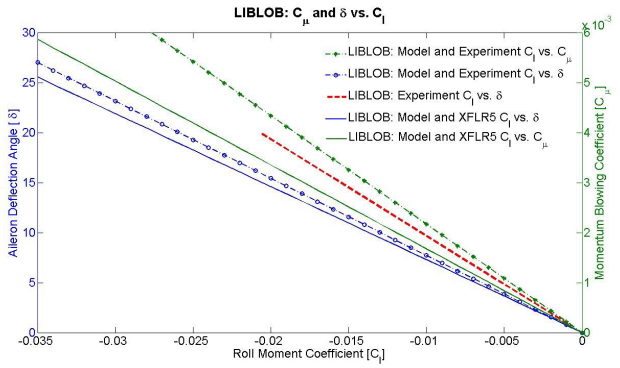

Figure 17. *Comparison between different rolling moments achieved with CC blowing and different rolling moments achieved with aileron deflection based on experimental results for full left wing actuator.*

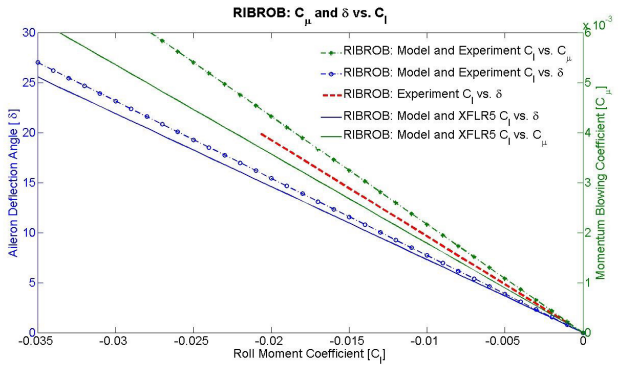

Figure 18. *Comparison between different rolling moments achieved with CC blowing and different rolling moments achieved with aileron deflection based on experimental results for full right wing actuator.*

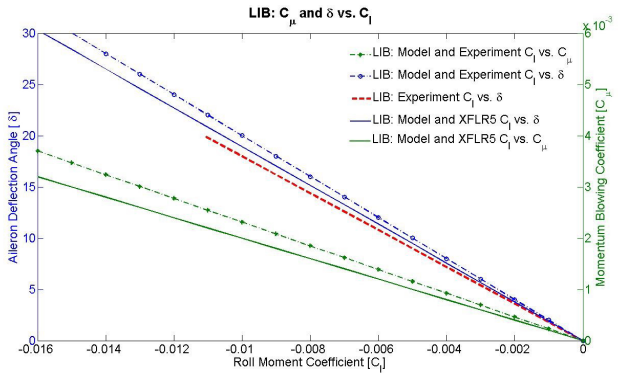

Figure 19. *Comparison between different rolling moments achieved with CC blowing and different rolling moments achieved with aileron deflection based on experimental results for inboard left wing actuator.*

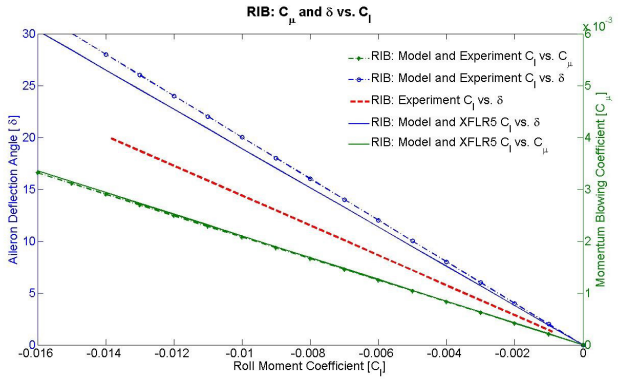

Figure 20. *Comparison between different rolling moments achieved with CC blowing and different rolling moments achieved with aileron deflection based on experimental results for inboard right wing actuator.*

on the circulation control effectiveness plot in Figure 7. Although based on the effectiveness plot, the Coanda surface geometry does not correspond to the region of maximum effectiveness due to compromise that had to be made to keep the jet flow subsonic.

The calculations were then carried out for a slot of 0.003m. All calculations used the experimental data or the XFLR5 predictions in combination with the semi-empirical model for roll control authority of the ailerons. The circulation control roll predictions were plotted against the aileron roll control data. The momentum blowing coefficient and aileron deflection angle were compared on the same graph versus the rolling moment that they produce. The predictions based on experimental data were placed in the same plots as the predictions based on XFLR5 to evaluate XFLR5's predictive abilities. The data for LIBLOB, RIBROB, LIB, and RIB ailerons is presented in figures 17-20.

E. Circulation Control Flow Requirements

The power requirements necessary to achieve CC were presented in terms of the maximum mass flow rate that is necessary to achieve a maneuver equivalent to 20˚ aileron deflection. The necessary momentum blowing coefficients and the corresponding mass flow rates for the ailerons were presented in Table III. Jett Exit Velocity values were calculated from the semi-empirical model using the experimental data. The air necessary for CC can be supplied from a separate compressor designed to feed the CC system or bled from the engine.

In the case of Demon, there was a 10% bleed mass flow requirement during cruise [Ref. 1] which could be met with 12% loss in thrust. This is a significant thrust penalty and thus a separate compressor for CC control was decided preferable. Demon has roughly twice the wing span of the SACCON wind tunnel model and uses AMT TITAN engine with sea level static thrust of

Aileron	C_u	$\dot{m}_j$ [kg/s]
LIBLOB	0.004486	0.013
RIBROB	0.004493	0.013
LIB	0.002572	0.0034
RIB	0.002883	0.0036

Table 3. *Mass Flow Rate Requirements for CC Equivalent to 20° Aileron Deflection*

392N, thus it is believed that SACCON designs which employ CC and have similar size and engine should use a separate compressor.

Discussion

A. Comparison of Experimental and Computational Results

The results show that the experimental data from the different tests is repeatable and reproducible with the exception of some minor differences in the region from 16° angle of attack onward. This is explained by the complex flow field around the geometry dominated by strong vortex-to-vortex and vortex-to-surface interactions . The linear portion of the lift curve where there is no separation can be closely reproduced by XFLR5. However, the pitching moment curve cannot be captured. State-of-the-art CFD codes used in NATO Task Groups also failed to reproduce the pitching moment behavior of SACCON. The reason is believed to be the vortex structures that form around the airframe. XFLR5, as expected, over predicted the rolling moment due to ailerons. The values had maximum of 57% error relative to the experimental results. The higher values for roll were due to the specifics of the potential flow theory which results in higher force estimates, the slightly bigger control surfaces modelled in XFLR5, and the software's lack of potential to capture separation which decreases the control surface effectiveness. In comparison, more advanced CFD codes also achieved significant errors for roll moment in the same flight envelope, which comes to show that even state-of-the art software has problems modelling the complex vortex flow (Fig. 14). Another thing that XFLR5 did not capture was the decreased effectiveness of the outboard ailerons. The NATO task groups found that, contrary to expectation, the inboard ailerons have higher influence on roll than the outboard ailerons. This was also explained with the vortex disturbed flow over the wing. The overall predictive ability of XFLR5 was considered good, given that it is a freeware, for lift and roll in the regions of small angles of attack, where the flow is undisturbed. The pitching moment predictions were not good but they closely matched some of the CFD software predictions. Thus, XFLR5 was concluded to be a good starting tool.

The semi-empirical equation gave about 20% over prediction for the full aileron roll moment control authority relative to the experimental data. However, the roll control authority for the inboard ailerons was under predicted. The effectiveness of the outboard aileron was over predicted due to inability of the equation to account for the vortex formation. Thus, the overall effect was a slight over prediction of the control effectiveness of the full ailerons.

B. Comparison of Circulation Control and Ailerons

The semi-empirical aileron roll control authority model was used to model both the aileron and the circulation control effectiveness (Eq. 4 and Eq. 10). Experimental data and XFLR5 predictions for the lift were used in the equations to obtain predictions for the roll moment due to aileron (blue lines in Fig. 17 through 20). The actual aileron response that was experimentally obtained by the NATO STO-AVT-201 task group was compared against the aileron model (red dashed line in Fig. 17 through 20). The maximum error between the semi-empirical model and the experimental data was found to be 32% for RIB aileron. However, the error for the other cases is on the order of 20%. This is not a small error, but is acceptable given that this is a first model which does not directly account for the possible disturbances created by the complex flow structures around SACCON. Furthermore, this model is able to directly compare the roll moment due to ailerons and due to circulation control. Thus, it was considered reasonable to apply the model.

Both the empirical model in combination with experimental data and the empirical model in combination with XFLR5 computations over predict the aileron control authority for LIBLOB and RIBROB ailerons, in the sense that according to the model, the same rolling moment is achieved

with a smaller aileron deflection angle compared to experimental data. The opposite is observed for the inboard ailerons – their performance is under predicted by the empirical model in both cases when experimental data and XFLR5 calculations were used. The model predicts that for the same roll moment a higher deflection angle is needed compared to the experiment. This result means that the effectiveness of the full aileron is lower than the one predicted by the model, and the effectiveness of the inboard ailerons is higher than the one predicted by the model. Calculations for the outboard aileron were not made due to the lack of experimental data for comparison. Assuming that the inboard and outboard aileron effects can be superimposed, meaning that the effect of the inboard can be added to the effect of the outboard aileron to obtain the effect of the full aileron, it was estimated that the actual effectiveness of the outboard aileron will be lower than the one that the model would predict. This is in agreement with the NATO STO-AVT-201 task group results that the outboard aileron has a decreased effectiveness.

The same model was used for the CC calculations, meaning that the error in the predictions would be on the same order as the error for aileron effectiveness. Thus, the expectation is that the effectiveness of the full span CC effectors would be over predicted by about 20%. In reality, this would result in a higher momentum blowing coefficient necessary to achieve the required roll moment.

C. Comparison to Demon

The FLAVIIR Demon UAV project was the first UAV to employ circulation control techniques to successfully achieve control in cruise. The CC model predictions developed and described in this paper were compared against the Demon UAV results. Figure 21 shows that the aileron deflection angle and momentum blowing coefficient necessary to achieve a rolling moment Cl=0.014 are 10˚ and 0.001, respectively. The predicted aileron deflection and momentum blowing coefficient values for SACCON to achieve rolling moment Cl=0.014 were 13˚ and 0.003. A comparison between the values for SACCON and Demon shows that the numbers are similar and of the same order of magnitude, which implies that the predictions for SACCON are realistic.

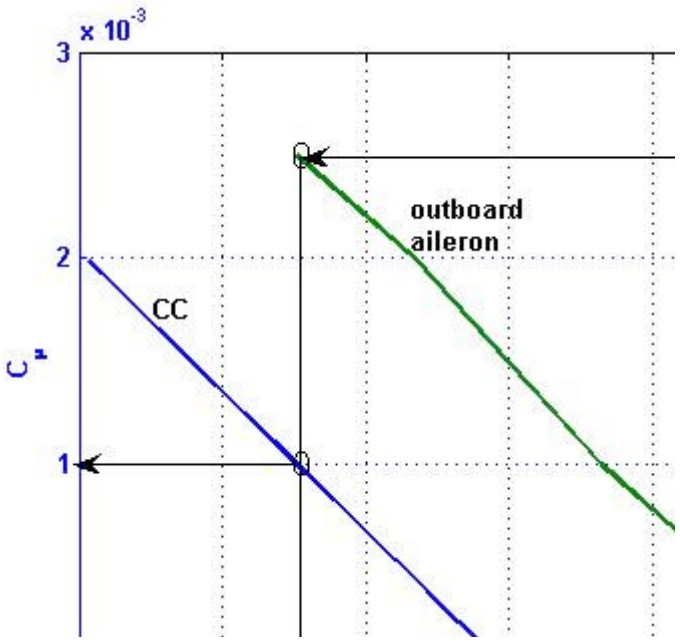

Figure 21. *Comparison of the differential rolling moment at different blowing setting with differential rolling moment achievable with mechanical aileron deflection for Demon UAV [Ref. 1].*

F. Future work

The semi-empirical model has no means of accounting for the vortex formations which affect the flow above the maneuver actuators. It is unclear what the influence of these vortices will have on the circulation control effectiveness. Therefore the error expectations discussed in the previous section need to be confirmed experimentally.

In order to confirm and correct, if needed, the circulation control model, a windtunnel experiment is being considered. The experiment is planned to be conducted in a transonic windtunnel, with the possibility of using the IIT supersonic windtunnel operated at subsonic regime. An airfoil with a Coanda surface has to be built and tested at cruise conditions. The experiment would investigate the validity of equations 2, 3, and 10, and figures 17 and 18. The hope is to obtain research funding from an appropriate funding agency to further explore the feasibility of Circulation Control as means of maneuver control for the SACCON airframe.

Considering that the IIT supersonic windtunnel will be available, a 4” by 2” airfoil fitted to the size of the test chamber of the tunnel will be used. The airfoil will be attached to a force transducer and placed in flow with Mach number

ranging from 0.5 to 0.8 in order to simulate cruise conditions. The sensitivity of the force balance can be obtained from ideal gas and isentropic flow relations:

$$P_0 = P\left(1 + \frac{\gamma - 1}{2} M^2\right)^{\frac{\gamma}{\gamma - 1}} \quad \text{Eq. 11}$$

$$T_0 = T\left(1 + \frac{\gamma - 1}{2} M^2\right) \quad \text{Eq. 12}$$

$$P = \rho RT \quad \text{Eq. 13}$$

where R is the individual ideal gas constant, ρ is density, T is temperature, P is pressure, M is Mach number, γ is the heat capacity ratio, and the subscript 0 indicates stagnation condition. The stagnation conditions in the pressure chamber of the wind tunnel are P0=25psia=170.2kPa and T0=300K. Using these relations, the test section conditions can be calculated to be P=170kPa, T=266K, and ρ=1.45kg/m3.

A symmetrical airfoil with lift coefficient CL=1.1 is going to produce a lift force L:

$$L = \frac{1}{2} \rho V_\infty{}^2 C_L S_w \quad \text{Eq. 14}$$

where the ρ is the density of the free stream air, V∞ is the free stream jet velocity, and Sw is the projected area. Given that the maximum Mach number in the test section will be 0.8, V∞=261.5m/s. A symmetrical airfoil with dimensions 4" by 2" will exert a force F=L=282.3N on the force transducer. Adding a factor of safety of 2 would mean that a force transducer that can withstand 600N will be needed. With a moment arm of 2", the maximum torque requirement will be 30Nm.

Conclusion

The goal of replacing mechanical control surfaces of airplanes with fluidic controls was investigated in this research. Circulation Control (CC) and its application to the SACCON airframe in order to produce rolling motion was the main objective. First, understanding the flow features around the airframe was achieved which was critical for developing understanding of the airframe performance issues. Software (XFLR5) based on potential flow theory was used to predict SACCON's performance and calculate the roll moments due to aileron deflections. The computational predictions were compared to experimental data. XFLR5 was incapable of adequately simulating the vortex structures and separation at high angles of attack, but this was not crucial for the applications of the project. Thus, it was concluded that the software had good predictive abilities as a first approximation of the real airframe. Circulation Control model was developed and applied to SACCON to show that it is possible to replace mechanical control surfaces with fluidic actuators. The results were used to predict the mass flow rate of air required to be supplied to achieve CC. Although experimentally unconfirmed, the model predictions were promising because they were in agreement with the results from the FLAVIIR project. Future work is necessary to validate the findings of the research. In order to confirm the predictive abilities of the model and make adjustments, a windtunnel experiment was designed and planned.

Acknowledgements

The author would like to acknowledge the help and support of the following people and organizations:

ACE Undergrad Research Program
For their financial support of this project

Professor David Williams
For his mentoring and help.

Lou Grimaud, Xuanhong An, Simeon Iliev, Camille Musquar
For being great coworkers and friends, introducing me to PIV, and for helping me learn about the GK Model.

Illinois Institute of Technology & Paul Galvin Library
For their support of this research.

References

[1] Buonanno, A., "Aerodynamic Circulation Control for Flapless Flight Control of an Unmanned Air Vehicle", PhD Thesis, Cranfield University, January 2009.

[2] Liersch, C., and Huber, K., "Conceptual Design and Aerodynamic Analyses of a Generic UCAV Configuration", AIAA Aviation, 32nd AIAA Applied Aerodynamics Conference: Atlanta, GA, USA, June, 2014.

[3] Cummings, R., and Schutte, A., "An Integrat-

ed Computational/Experimental Approach to UCAV Stability & Control Estimation: Overview of NATO RTO AVT-161", AIAA, NATO RTO-AVT-161, 2010.

[4] Lofthouse, A., Ghoreyshi, M, Cummings, R., and Young, M., "Static and Dynamic Simulations of a Generic UCAV Geometry Using the Kestrel Flow Solver", AIAA Aviation, 32nd AIAA Applied Aerodynamics Conference: Atlanta, GA, USA, June, 2014.

[5] Englar, R. J., "Circulation Control for High Lift and Drag Generation on STOL Aircraft," Journal of Aircraft, vol. 12, no. 5, pp. 457–463, 1975.

[6] Kind, R. J. "An Experimental Investigation of a Low Speed Circulation Control Airfoil", The Aeronautical Quarterly, Vol. XIX, pp.170-182, 1968.

[7] Loth, J. L., and Boasson, M., "Circulation Controlled STOL Wing Optimization", Journal of Aircraft, vol. 21, no. 2, 1984.

[8] Chard, J., Jegede, O., Llopis-Pascual, A., and Crowther, W., "Towards High Speed Fluidic Flight Controls", University of Manchester, NATO STO-MP-AVT-215.

[9] Englar, R.J.; David, W. "Two-Dimensional Subsonic Wind Tunnel Tests of Two 15-Precent Thick Circulation Control Airfoils", Technical Note AL-211, Taylor Naval Ship Research and Development Center: Washington, DC, USA, 1971.

[10] Shires, A. and Kourkoulis, V., "Application of Circulation Controlled Blades for Vertical Axis Wind Turbines", Energies, July, 2013.

[11] Sadraey, M., "Aircraft Design: A Systems Engineering Approach", Wiley Publications, September 2012.

[12] Frink, N., Tormalm, M., and Schmidt, S., "Unstructured CFD Aerodynamic Analysis of a Generic UCAV Configuration", NATO RTO-MP-AVT-170, Paper no. 25. [13] Huber, K., Vicroy, D., Schutte, A., and Hubner, A.-R., "UCAV model design and static experimental investigations to estimate control device effectiveness and Stability and Control capabilities", AIAA Aviation, 32nd AIAA Applied Aerodynamics Conference: Atlanta, GA, USA, June, 2